02

Wave-diffusion delivery of the HIF-1α protein onto COOH-MWCNTs and regulation of oxygen in biocells

© N.G. Bobenko,[1] V.V. Shunaev,[2] V.E. Egorushkin,[1] O.E. Glukhova[2]

[1] Institute of Strength Physics and Materials Science, Siberian Branch, Russian Academy of Sciences,
634055 Tomsk, Russia
[2] Department of Physics, Saratov State University,
410012 Saratov, Russia
e-mail: nbobenko@ispms.ru

Received December 22, 2023
Revised December 22, 2023
Accepted December 22, 2023

Carboxyl-functionalized nitrogen-doped multiwalled carbon nanotubes (COOH-N-MWCNTs) have been successfully used for the delivery of various drugs, genes and proteins. Delivery and controlled release of the HIF-1α protein from the carrier is an important task, since its deficiency or excess leads to the development of hypoxia, cancer, cardiovascular and other diseases. Using the so-called self-consistent-charge density-functional tight-binding method and the quantum equations of motion, it was performed modeling and analysis of the electron-energy properties of the COOH-N-MWCNT/HIF-1α complex, it was determined the structural conditions for the effective attachment and delivery of the HIF-1α protein, it was described the conditions for wave diffusion during delivery and regulation of oxygen concentrations by the HIF-1α protein in biocells. It has been shown that the hybridization of electronic states plays a major role in diffuse relaxation, oxygen regulation, and the possibility of drug delivery. The nature of wave diffusion is determined by the hybridization of the $-$OH group of the HIF-1α protein and the carboxyl group of COOH-N-MWCNTs.

Keywords: carbon nanotubes, hypoxia-induced factor HIF-1α, carboxyl group, electron density functional method in the tight binding approximation, method of quantum equations of motion, wave diffusion.

DOI: 10.21883/0000000000

Introduction

In recent decades, all over the world there has been an increase in diseases caused by impaired oxygen metabolism in the human body [1]. Oxygen concentration can be regulated by introducing the protein hypoxia-induced factor 1-alpha (HIF-1α). In 2019 the Nobel Prize in Medicine was awarded for the discovery of the mechanism of regulation of hypoxia by the HIF-1α protein. In particular, the influence of HIF-1α on the activity of genes that change the number and intensity of mitochondria, oxygen transfer and production has been established [2]. In addition, HIF-1α can also act as a carrier for other drugs and a „target" for additional chemotherapy for cancer and other diseases. Researchers all over the world are working on the task of targeted delivery of HIF-1α to individual organs, tissues and biocells.

The unique properties of carbon nanotubes (CNT), such as a high surface-to-volume ratio, increased strength, biocompatibility, ability to be functionalized, etc., make them promising in biomedicine, drug, protein and gene delivery [3–5]. CNT are effectively absorbed by various types of cells and are already used as carriers of antitumor molecules, anti-inflammatory drugs, osteogenic steroids dexamethasone, etc. [6]. Functionalization of the CNT surface has allowed to use them for the delivery of various genes, such as plasmid DNA, micro-RNA and small interfering RNA, etc. The use of CNT as a carrier of biologically active substances increases the half-life of drugs in humans and facilitates their delivery directly to target cells [7]. CNT with attached COOH groups are promising platforms for the delivery of many drugs, and HIF-1α in particular.

Currently , several methods have been proposed to control the efficiency of loading and delivery of drugs into the structures of multi-wall CNT (MWCNT): varying the methods of drug impregnation, additional modification of the surface with various functional groups, etc. However, the current lack of information on the fundamental aspects of controlling the key mechanisms that ensure the applicability of MWCNT as drug carriers hinders the development of targeted drug delivery systems based on them.

Experimental studies on the attachment of HIF-1α to nitrogen-doped MWCNT functionalized with carboxyl groups (COOH-N-MWCNT) and determining the role of carboxyl functionalization have not yet been carried out, however, it was found that the addition of siRNA/O CNT leads to a strong inhibition of the cellular activity of HIF-1α [8], and the addition of oxidized N-SWNTs — decreases the expression of the HIF-1α protein [9]. Increasing the concentration of oxygen delivered to cells by single-walled nanotubes also increases the number of HIF-1α-driven proteins involved in apoptosis, autophagy, cell survival and growth [9].

For the rapid implementation of local drug delivery systems based on MWCNT, it is required to understand the mechanism of regulation of HIF-1α oxygen concentration in the body. Changes in the concentration of drug released from the carrier due to normal diffusion depend linearly or exponentially on time [10,11]. However, wave kinetics of drug release has also been discovered experimentally for proteins [12]. The mechanism of wave diffusion yield has not yet been explained. In this regard, the purpose of this work is to determine the mechanism of formation of the COOH-N-MWCNT/HIF-1α complex, as well as the possibility of wave diffusion during the delivery and regulation of oxygen concentration by the HIF-1α protein in biocells.

1. Experimental

To construct the atomic structures of the objects under consideration and analyze their electron-energy properties, the electron density functional method was used in the strong coupling approximation with self-consistent calculation of the charge SCC DFTB [13]. The method was previously successfully used by the authors to simulate the process of functionalization of graphene with oxygen-containing groups and transition metal oxides [14,15]. As part of this method, the total energy of the structure E_{tot} is found as the sum of the energy of the band structure E_{BS}, the repulsion energy E_{rep} and the energy of the self-consistent charge E_{SCC}:

$$E_{tot} = E_{BS} + E_{rep} + E_{SCC}. \quad (1)$$

The interaction of C, N, O, and H atoms was described by the 3ob-3-1 basis set of parameters developed for biological and organic molecules [16]. The search for equilibrium structures was carried out by minimizing the total energy (1) over atomic coordinates using the conjugate gradient method at an electron temperature of 300 K, until the force acting on the atom did not exceed $1E^{-4}$ eV/atom. To calculate the band structure, the reciprocal space partitioning was applied by the Monkhorst-Pack method with the $16 \times 16 \times 1$ grid.

The charge distribution on the atoms was calculated using the Mulliken procedure [17], according to which the charge on each of the atoms Z is equal to:

$$Z = Z_A - GAP_A, \quad (3)$$

where Z_A — atomic number in the Periodic Table, and GAP_A — the total charge on the orbitals belonging to atom A.

The bond energy E_b between objects M and N was found according to the classical formula:

$$E_b(M + N) = E(M + N) - E(M) - E(N), \quad (4)$$

where $E(M)$ and $E(N)$ — energies of objects M and N in an isolated state, $E(M + N)$ — energy after bond formation.

The method of quantum equations of motion was used to develop the theory of hybridization and degradation kinetics of the COOH-N-MWCNT-HIF1α system, to determine the structural conditions for effective attachment and delivery of the HIF-1α protein, by specifying the nature of chemical bonds and the dynamics of their change. This method is applied in theories of chemical bonding and decomposition [18].

2. Results and discussions

2.1. Studies by SCC DFTB method

The diameter of the majority of synthesized MWCNT exceeds 10 nm, and therefore small areas of external CNT can be considered flat and modeled as monolayer graphene. The lattice cell of the surface of carboxyl-functionalized nitrided COOH-N-MWCNT was a graphene sheet and was constructed on the basis of experimental data on the structure obtained by XPS, NEXAFS, and Raman methods [19] (Fig. 1, *a*). This cell contains 6% oxygen atoms located in the carboxyl and carbonyl groups, one Stone-Wells defect, and one substitutional nitrogen. It is known that such a concentration of oxygen-containing groups leads to the formation of long-range ordered structures [19], which determines the presence of boundary conditions in the form of translation to infinity in two directions L_x and L_y. To attach three molecules of HIF-1α ($C_{26}H_{29}NO_5$), indicated by blue atoms in Fig. 1, *b* [20], the lattice cell of MWCNT (gray atoms) was expanded. Numerical experiments determined the most advantageous attachment sites for the protein. The highest bond energy in modulus (-0.64 eV) was observed in the case of two hydrogen bonds $-$OH of the protein with the elements $-$OH and $-$O of the carboxyl group of MWCNT. In this case, the length of the OH$-$OH bond was 1.876 Å, OH$-$O — 1.936 Å.

Figure 2 shows graphs of the density of electronic states (DOS) and partial DOS of the COOH-N-MWCNT/HIF-1α complex. Fermi level of the $E_F = -4.73$ eV system (Fermi level of the COOH-N-MUNT -4.48 eV lattice cell). The electronic states of HIF-1α are separated by the energy slit ~ 3 eV against the background of an overall high density of states. The energy positions of the peaks (Table 1) of the partial DOS of HIF-1α and COOH-N-MWCNT do not coincide, which indicates their weak hybridization (Fig. 2, *a*). This is also confirmed by the partial DOS $-$OH and $-$O of the MWCNT and $-$OH groups of the protein connected by hydrogen bonds: peaks *1* and *3* in the $-$OH zone of the protein are located significantly lower in energy from the peaks *2* and *4* $-$OH tubes. The $-$O peak (peak *4*) is due to the second bond of the $-$OH protein with the $-$O carboxyl (Fig. 2, *b*).

Let us analyze the charge transfer between the protein and the carboxyl based on Table 2, which illustrates the redistribution of charge on individual atoms after the formation of the complex. It follows from the table that $-$OH of MWCNT carboxyl donates 0.01e of $-$OH of

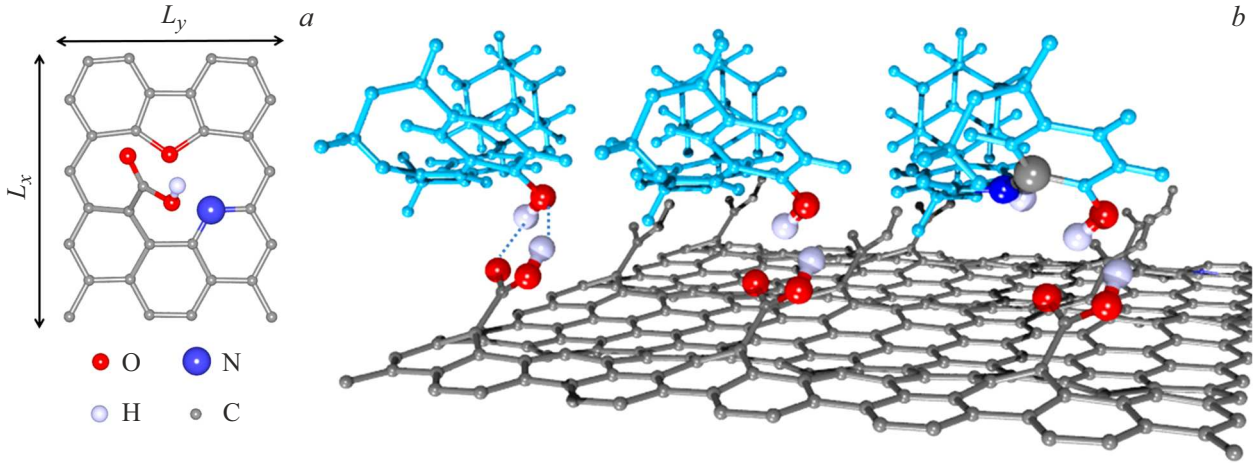

Figure 1. *a* — unit cell COOH-N-MWCNT; *b* — surface of COOH-N-MWCNT (gray atoms) with attached HIF-1α protein molecules (blue atoms). On the right molecule of the protein, nitrogen, carbon, and hydrogen atoms are highlighted, which play a key role in the redistribution of charge within the system.

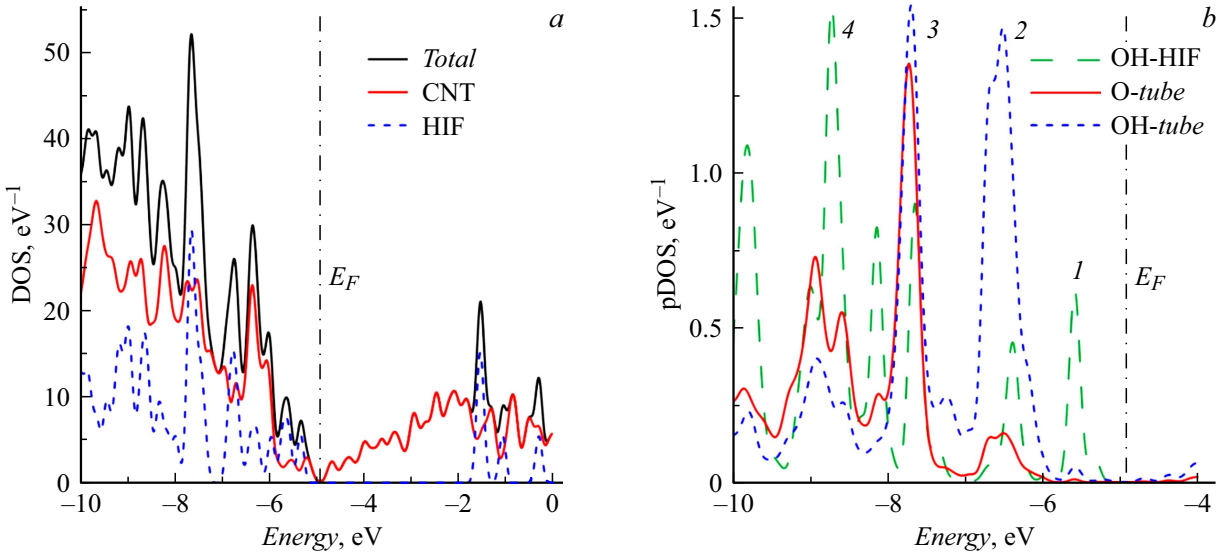

Figure 2. DOS of the components of the COOH-N-MWCNT/HIF-1α system: *a* — full DOS; *b* — partial DOS.

Table 1. Positions of pDOS HIF-1α and carboxyl peaks and their energy differences (ω)

Peak number				
1	*2*	*3*	*4*	ω
−5.58(HIF -OH)	−6.60(tube -OH)	−6.39(HIF -OH)	−6.59(tube -O)	1.02 (1−2) 0.20 (3−4)

Table 2. Charge redistribution on individual COOH-N-MWCNT and HIF-1α atoms during bond formation

HIF-1α			COOH-N-MWNT			
OH	O	C	OH	N	C	H
−0.02e	+0.05e	−0.01e	+0.01e	−0.01e	−0.01e	−0.01e

*Note**: The atoms listed in the table are highlighted in Fig. 1, *b*

protein. The carboxyl oxygen of the protein takes away the rest of the flowed charge: 0.01e each from the C and −OH atoms of the MWCNT carboxyl, as well as from the C, N, H — atoms of the nearest donor atoms of the protein indicated in Fig. 2. Let us note that it is not the nearest carbon atom bonded to the O-protein atom that transfers the charge, but the C atom highlighted in Fig. 1, *b*. This may be due to the influence of the N atom, which increases the charge of the nearby C atom, which transfers the charge to the O atom from the carboxyl.

2.2. Studies by the method of quantum equations of motion

The calculations show that in all processes of functionalization and bond formation, the main role is played by hybridization and charge transfer. Let us review the dynamics of hybridization using the method of quantum equations of motion.

Let us review the interaction of the HIF-1α molecule with a functionalized nanotube, leading to the formation of new chemical bonds. These processes are associated with the hybridization of electrons of the protein and the carboxyl complex and can be studied within the framework of the standard Hamiltonian in the secondary quantization representation (for one spin subband):

$$H = \Sigma_l \varepsilon_l c_l^+ c_l + \Sigma_n \varepsilon_n a_n^+ a_n + \Sigma_{e,n} V_{en}(c_l^+ a_n + a_n^+ c_l), \quad (5)$$

where $c_l^+(c_l)$, $a_n^+(a_n)$ — operators of creation and destruction of electrons of the protein and carboxyl group in the Vanier representation, ε_l, ε_n — electron energies relative to the Fermi level, V_{ln} — hybridization matrix elements, n, l determine the position of the atoms. Let us write down the equations of motion

$$\dot{c}_l^+ = i[Hc_l^+], \ \dot{a}_n^+ = i[Ha_n^+], \quad (6)$$

where $[\ldots]$ — commutators. Performing simple transformations, we obtain the following system of equations:

$$\ddot{c}_l + \gamma \dot{c}_l + \Sigma_n |V_{ln}|^2 c_l^+ = \Sigma_n V_{ln} \omega_{ln} e^{-\omega_{ln} t} a_n^+, \quad (7)$$

$$\ddot{a}_n^+ + \Sigma_k |V_{kn}|^2 a_n^+ = \Sigma_k (\omega_{kn} - i\gamma) e^{\omega_{kn} t} c_k^+, \quad (8)$$

where $\omega_l n = \varepsilon_l - \varepsilon_n$ (in units), γ — attenuation of the c_l^+ mode due to hybridization. These two processes represent two coupled oscillatory processes, where V and ω play the roles of natural and forced frequencies, respectively.

To find a solution to equation (8) with a two-mode approximation in the form $a_n^+ = \rho e^{i\omega t}$, we express a_n^+ from equation (8) and substitute it into equation (7):

$$\ddot{c}_l^+ + \gamma \dot{c}_l^+ + V^2 \frac{V^2 + i\gamma\omega}{V^2 - \omega^2} c_l^+ = 0, \quad (9)$$

where $V \equiv V_{ln}$, $\omega \equiv \omega_{ln}$. This equation describes reactive (oscillatory) and relaxation motion in terms of average values. Both in form and content, equation (9) is identical to the phenomenological equation of motion for fluctuations of the „order parameter“ [21] for the electron density c_l^+ of a molecule. Therefore, the coefficient in front of c_l^+ in equation (9) is the inverse susceptibility (χ^{-1}) in a given state of the system. As is known, the value χ^{-1} corresponds to the square of the frequency Ω^2 of the dynamic mode of the molecule [21].

If $V > \omega$, $\Omega^2 = \frac{V^4 + i\gamma V^2}{V^2 - \omega^2}$, then the values V, ω and their ratio determine the reactivity of the surface in relation to the vibrational behavior of the molecule.

But in addition to the $V > \omega$ case, which corresponds to the location of the molecule near the surface, there is the possibility of the $\omega > V$ state, when the protein is far from the surface. Here hybridization and charge transfer are small. To illustrate the above, the electron density distribution is shown in Fig. 3.

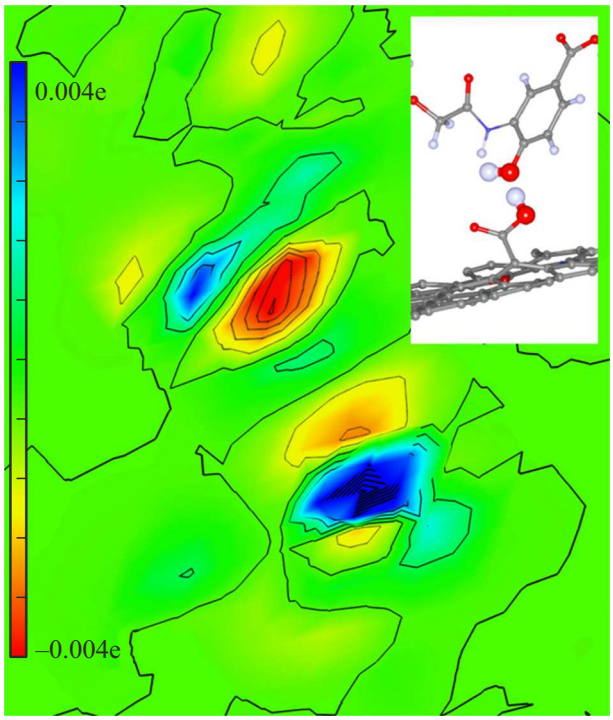

Figure 3. Electron density distribution near the COOH-N-MWCNT bond and HIF-1α. The spatial atom arrangement for which the electron density distribution is shown is presented in the inset.

For these states of hybridization γ are small (Fig. 3) and

$$\Omega = i \frac{V^2}{\sqrt{\omega^2 - V^2}}. \quad (10)$$

Equation (10) represents a relaxation, diffusion mode, and the molecule moves in a hydrodynamic node, where its vibrational density is $\delta n \sim e^{i(\Omega t - \vec{q}\vec{r})}$ with $\Omega = iDq^2$ [22]. Thus, $\delta n \sim e^{-t/\tau}$, $\frac{1}{\tau} = Dq^2$ (D — diffusion constant). According to the equation (10):

$$D = \frac{V^2}{q^2 \sqrt{\omega^2 - V^2}}. \quad (11)$$

The behavior of the molecule in this state is wave-like diffusion, in which density is transferred from regions with excess to regions with deficiency in protein density at a distance of wavelength $\lambda \sim \frac{2\pi}{q}$ (q — vector near the K-point of the Brillouin zone). Diffusion constant D depends only on V, ω and their ratio. If $V \to \omega$, then the constant D increases. The diffusion ability of the protein associated with carboxyl complexes and drug release are also increased. In diffusion control models [23] the ratio between the number of released protein M_1 and M_2 over time t has

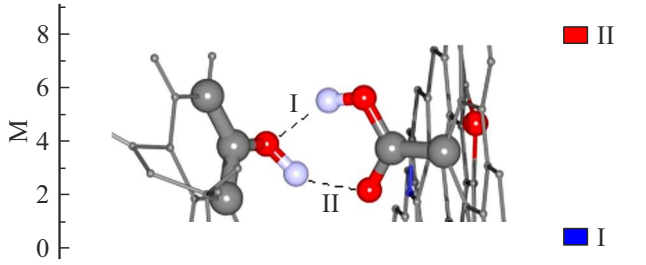

Figure 4. Opportunity of yield of HIF-1α from the surface of COOH-N-MWCNT due to OH-OH (I) and OH-O (II) bonds.

the form

$$\frac{M_2}{M_1} = \frac{D_2^2}{D_1^2} = \left(\frac{V_2}{V_1}\right)^4 \frac{(\omega_1^2 - V_1^2)}{(\omega_2^2 - V_2^2)}. \quad (12)$$

In case $\omega \gg V$ and $V_2 \sim V_1$:

$$M_2 \sim M_1 \frac{\omega_1^2}{\omega_2^2}, \quad (13)$$

where M_2 — release over time t_2, M_1 — release over time t_1. Since ω depends on the protein concentration (c), we can calculate $M_2(c)$ by varying ω depending on the concentration and taking $M_1 = 1$ (Fig. 4).

When a HIF-1α molecule hybridizes with a carboxyl at 6% oxygen, two bonds arise (inset in Fig. 3) and, accordingly, two values ω: ω_{12} and ω_{34} (Table 1). The value ω_{12} refers to the OH-OH bond, and ω_{34} — to the OH-O bond. The value ω_{34} corresponding to the OH-O bond turns out to be significantly less than ω_{12}. This leads to two opportunities for changing protein yield (Fig. 4). The first opportunity at corresponds to a decrease M with increasing concentration (13), and the second, at ω_{34} — its increase (13). The first yield is possible with small amounts of oxygen, and the second one — with its excess. Since the behavior of molecules and the possible yield are determined only by the bond of the $-$OH group of the HIF-1α molecule with $-$OH and $-$O of the carboxyl, the excess oxygen can also be due to other circumstances, for example, when HIF-1α bonds with $-$O and $-$OH cells (hypoxia, cancer, etc.). In this case, the behavior of M determines the mechanism for regulating the relationship between HIF-1α and oxygen in cells: with a lack of oxygen (OH-OH bond), the yield of HIF-1α from the cell remains almost unchanged with increasing concentration, and with an excess of oxygen (OH-OH bond) O) — the yield increases. This is precisely the effect observed experimentally [2].

Conclusion

In this work, we studied the interaction of HIF-1α proteins with MWCNT functionalized with carboxyl groups. As a result of a series of quantum mechanical calculations, the optimal landing sites for protein structures, as well as the ground type of bond (hydrogen), were determined. The charge redistribution between protein atoms and COOH-N-MWCNT was calculated, and the theory of hybridization and degradation kinetics of the COOH-N-MWCNT-HIF1α system was developed. It has been shown that the wave diffusion mechanism and the opportunity of regulating the oxygen concentration are determined by the characteristics of the electronic structure, hybridization and chemical bond of HIF-1α and COOH-N-MWCNT. Moreover, depending on the excess or lack of oxygen, the hydroxyl group of HIF-1α forms chemical bonds with either hydroxyl (OH-C) or carbonyl OH-(O=C) groups, respectively. The formation of predominantly bonds of one or another type between HIF-1α and oxygen-containing groups may be responsible for the hypoxia or normoxia that occurs in biocells.

Funding

The work by N.G. Bobenko and V.E. Egorushkin was performed as part of the state assignment of the Institute of Strength Physics and Materials Science of the Siberian Branch of the Russian Academy of Science, topic number FWRW-2022-0002. The work by V.V. Shunaev and O.E. Glukhova was performed with the financial support of the Ministry of Education and Science of Russia as part of the Government Task (project № FSRR-2023-0008).

Conflict of interest

The authors declare that they have no conflict of interest.

References

[1] M. Nakane. J. Intensive Care, **8**, 95 (2020). DOI: 10.1186/s40560-020-00505-9
[2] Z. Qing, Y. Qin, Y. Haifeng, W. Wenyi. Genes. Dis., **6** (4), 328 (2019). DOI: 10.1016/j.gendis.2019.10.006
[3] H. Zare, S. Ahmadi, A. Ghasemi, M. Ghanbari. Int. J. Nanomed, **16**, 1681 (2021). DOI: 10.2147/IJN.S299448
[4] R. Jha, A. Singh, P.K. Sharma, N.K. Fuloria. J. Drug Deliv. Sci. Technol., **58**, 101811 (2020). DOI: 10.1016/j.jddst.2020.101811
[5] M. Darroudi, S.E. Nazari, P. Kesharwani, M. Rezayi, M. Khazaei, A. Sahebkar. *Emerging Applications of Carbon Nanotubes in Drug and Gene Delivery* (Elsevier Ltd., 2023)
[6] A.K. Mehata, A. Setia, Vikas, A.K. Malik, R. Hassani, H.G. Dailah, H.A. Alhazmi, A.A. Albarraq, S. Mohan, M.S. Muthu. Pharmaceutics, **15**, 722 (2023). DOI: 10.3390/pharmaceutics15030722
[7] B.O. Murjani, P.S. Kadu, M. Bansod, S.S. Vaidya, M.D. Yadav. Carbon Lett., **32**, 1207 (2022). DOI: 10.1007/s42823-022-00364-4
[8] G. Bartholomeusz, P. Cherukuri, J. Kingston, L. Cognet, R. Lemos, T.K. Leeuw, L. Gumbiner-Russo, R.B. Weisman, G. Powis. Nano Res., **2**, 279 (2009). DOI: 10.1007/s12274-009-9026-7
[9] Y. Wang, C. Wang, Y. Jia, X. Cheng, Q. Lin, M. Zhu, Y. Lu, L. Ding, Z. Weng, K. Wu. PLoS ONE, **9**, e104209 (2014). DOI: 10.1371/journal.pone.0104209

[10] D. Chudoba, M. Jażdżewska, K. Łudzik, S. Wołoszczuk, E. Juszyńska-Gałazka, M. Kościński. Int. J. Mol. Sci., **22**, 12003 (2021). DOI: 10.3390/ijms222112003
[11] J.M. Tan, S. Bullo, S. Fakurazi, M.Z. Hussein. Sci. Rep., **10**, 16941 (2020). DOI: 10.1038/s41598-020-73963-8
[12] K.A. Prosolov, E.G. Komarova, E.A. Kazantseva, A.S. Lozhkomoev, S.O. Kazantsev, O.V. Bakina, M.V. Mishina, A.P. Zima, S.V. Krivoshchekov, I.A. Khlusov, Y.P. Sharkeev. Materials, **15**, 4643 (2022). DOI: 10.3390/ma15134643
[13] M. Elstner, D. Porezag, G. Jungnickel, J. Elsner, M. Haugk, Th. Frauenheim, S. Suhai, G. Seifert. Phys. Rev. B, **58**, 7260 (1998). DOI: 10.1103/PhysRevB.58.7260
[14] V. Shunaev, O. Glukhova. Lubricants, **10** (5), 79 (2022). DOI: 10.3390/lubricants10050079
[15] V.V. Shunaev, O.E. Glukhova. Membranes, **11** (8), 642 (2021). DOI: 10.3390/membranes11080642
[16] M. Gaus, A. Goez, M. Elstner. Chem. Theory Comput., **9** (1), 338 (2012). DOI: 10.1021/ct300849w
[17] R.S. Mulliken. J. Chem. Phys., **23**, 1833 (1995). DOI: 10.1063/1.1740588
[18] A.I. Baz', Ya.B.A. Zel'dovich, A.M. Perelomov. *Rasseyanie, reaktsii i raspady v nerelyativistskoy kvantovoy mekhanike* (Nauka, M., 1971) (in Russian)
[19] A.A. Belosludtseva, N.G. Bobenko, V.E. Egorushkin, P.M. Korusenko, N.V. Melnikova, S.N. Nesov. Synth. Met., **280**, 116866 (2021). DOI: 10.1016/j.synthmet.2021.116866
[20] Electronic media. *National Center for Biotechnology Information. PubChem Compound Summary for CID 16124726.* Available at: https://pubchem.ncbi.nlm.nih.gov/compound/lw6 (Accessed Nov. 25, 2022)
[21] E.M. Lifshitz, L.P. Pitaevskii. *Physical Kinetics* (Pergamon, London, UK, 1981)
[22] D. Forster. *Hydrodynamic Fluctuations, Broken Symmetry, and Correlation Functions* (CRC Press: Boca Raton, FL, USA, 2018)
[23] Y. Fu, W.J. Kao. Expert Opin Drug Deliv., **7**, 429 (2010). DOI: 10.1517/17425241003602259

Translated by A.Akhtyamov